Theoretical Developments and Experiments on the Multiple Anomalous Transmission of X Rays

ANDREW L. DALISA* AND ALFRED ZAJAC
Adelphi University, Garden City, New York

AND

CHIU HUNG NG
Polytechnic Institute of Brooklyn, Brooklyn, New York

(Received 26 May 1967; revised manuscript received 25 October 1967)

The modes of propagation of x rays for a four-beam case in the germanium crystal are evaluated, and, after the application of the proper boundary conditions, the ratios of the exit intensities are calculated. On the assumption that pairs of beams within modes form standing waves, the anomalously transmitted beams have been obtained. These results were subjected to experimental checks which seem to justify them. In addition, the actual forms of the dispersion sheets were obtained for a three-beam case in germanium. It was also shown that the symmetry points of the dispersion sheets play a dominant role in the anomalous transmission.

I. INTRODUCTION

THIS paper contains the results of the theoretical and experimental investigations of the multiple anomalous transmission of x rays which form a continuation and further development of the results obtained previously.[1–7] In these developments, the problem of evaluating the modes of propagation of electromagnetic waves in the crystal was of central importance. Such an evaluation leads to the possibility of a complete analysis of the multiple diffraction within the framework of the dynamical theory of x-ray diffraction.

This procedure was applied to a four-beam case in germanium (three simultaneous diffractions). All the normal modes were evaluated, the anomalously transmitted fields were calculated, and the results checked experimentally. The anomalously transmitted beams were obtained by determining the possible standing waves out of the various component fields, with nodes at the atomic planes. We did not include in our considerations absorption; to this extent, therefore, our experimental results would be expected to deviate from the calculated intensities.

In determining theoretically the anomalously transmitted fields, we first asked ourselves which of the eight modes are anomalously transmitted; this led to an investigation of the coupling of the various beams within any particular mode; it turns out that (within a mode) fields combine in pairs to produce anomalous transmission.

The importance of the surface of dispersion in the dynamical theory of x-ray diffraction is well realized. We have obtained and plotted the actual form of the intersection of the dispersion surface with three coordinate planes in a three-beam case in germanium.

For practical reasons, when applying the formalism of the modes of propagation to multiple diffraction, it is necessary to work with symmetry points of the dispersion surface. It is then, of course, important, to have an additional argument that these points are of primary importance in the anomalous transmission.

* Present address: U. S. Army, Fort Monmouth, N. J. Most of the work reported here has been performed by the first named author in partial fulfillment of the requirements for the Ph.D. degree at the Physics Department of Adelphi University. This work was in part supported by a multidisciplinary grant from NASA, and by a grant from the Research Corporation.

[1] E. J. Saccocio and A. Zajac, Acta Cryst. **18**, 478 (1965).

[2] E. J. Saccocio and A. Zajac, Phys. Rev. **139**, A255 (1965). The present paper is an extension of the results published in this paper and in Ref. 1. In addition, reference should be made to other related publications listed below (Refs. 3–6).

[3] E. Fues, Z. Physik **109**, 236 (1938).

[4] K. Kambe, J. Phys. Soc. Japan **12**, 13 (1957).

[5] G. Borrmann and W. Hartwig, Z. Krist. **121**, 401 (1965).

[6] G. Hildebrandt, Phys. Status Solidi **15**, K131 (1966).

[7] After the completion of the work reported here, we learned about the article of Joko and Fukuhara [J. Phys. Soc. Japan **22**, 597 (1967)]. These authors deal with several cases of simultaneous diffractions in germanium, viz., 000, 11$\bar{1}$, 111; 000, 202, 220; 000, 220, 400, 2$\bar{2}$0; and 000, 220, 242, 044, $\bar{2}$24, $\bar{2}$02. Of these, the second case is the same as that dealt with in Ref. 3, and the third case is the same as the one reported here. A comparison of the results contained in that paper and those reported here, as well as in Ref. 3, is in order. All these papers deal with the evaluation of the eigenvectors for the various cases of simultaneous diffraction. The eigenvectors belonging to distinct eigenvalues should, of course, be the same. In the work reported here, the only distinct eigenvalues are x_1 and x_2. Our modes agree with those obtained by Joko and Fukuhara. The apparent difference in sign in mode 2 results from different choice of unit vectors. (Our Fig. 2 should be compared with the diagram drawn at the bottom left of their Fig. 2.) The method of evaluating the eigenvectors corresponding to the degenerate eigenvalues differs here from that of Joko and Fukuhara. We have used a perturbation technique, and they simply added an orthonormalizing relation. Ours is a much more involved method, but perhaps appealing more to the physics of the problem; theirs is a much simpler and mathematically more elegant one. In the case of degenerate eigenvalues the eigenvectors may not have the same form, but their sum should be the same. In addition, any one eigenvector belonging to the degenerate eigenvalue should be expressible as a linear combination of all other eigenvectors belonging to the degenerate eigenvalue. Under these considerations the results presented here, as well as in Ref. 3, are essentially the same as the corresponding cases treated by Joko and Fukuhara. It has to be stressed that these authors include in their treatment the problem of absorption explicitly, and in this way they predict the anomalous transmission of x rays. We arrive at the anomalous transmission by looking at the fields which produce standing waves along the atomic planes; we are not including absorption in our treatment.

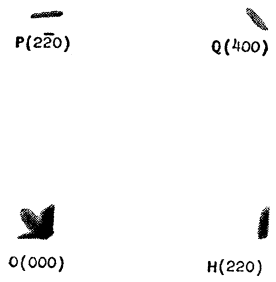

FIG. 1. A photograph of four anomalously transmitted beams.

We furnish such an argument which then justifies the procedure of evaluating the normal modes at the symmetry points only, and, as already stated, such an evaluation simplifies the entire problem considerably.[8]

II. FOUR-FIELD SOLUTION

A. General Theory

In the general dynamical theory, one assumes wave solutions to Maxwell's equations in the form of Bloch functions

$$\mathbf{E}=e^{2\pi i\nu t}\sum_H \mathbf{E}_H e^{-2\pi \mathbf{k}_H\cdot\mathbf{r}},$$

where $\mathbf{k}_H$ is the wave vector directed towards the reciprocal lattice point H.[9,10] This leads to a set of vector equations that describe the permitted electric fields in the crystal and which are of the form

$$x_H\mathbf{E}_H+\sum_{H\neq J}\phi_{H-J}\mathbf{E}_J=0, \tag{2.1}$$

where x_H is defined by the relation

$$k^2x_H=k_H{}^2-k^2(1-\phi_0). \tag{2.2}$$

ϕ_{H-J} is the Fourier component of the polarizability and is given by

$$\phi_H=A\sum_j f_j e^{-2\pi i\rho_H\cdot\mathbf{r}}. \tag{2.3}$$

Here ρ_H designates a reciprocal-lattice vector. We notice that

$$\phi_H=AF_H,$$

i.e., ϕ_H is proportional to the geometrical structure factor.

The transverse electric-field vectors $\mathbf{E}_H$ can be expressed in terms of two components $E_H{}^\sigma$ and $E_H{}^\pi$ along the unit vectors $\boldsymbol{\sigma}_n$ and $\boldsymbol{\pi}_n$ in the plane transverse to $\mathbf{k}_H$.

B. Participating Reflections

A four-beam case in germanium that exhibits strong anomalous transmission is that of $O(000)$, $H(220)$, $P(2\bar{2}0)$, and $Q(400)$. Figure 1 is a reproduction of a photograph of the four x-ray beams forming this particular set of simultaneous anomalous transmission. For the purpose of this photograph, the incident beam was made divergent deliberately, so that one can clearly see that each diffracted beam has a corresponding beam diffracted in the incident direction.

The four points O, H, P, and Q are situated at the corners of a square in the reciprocal-lattice space. The unit vectors $\boldsymbol{\sigma}$ and $\boldsymbol{\pi}$ chosen at each wave vector are shown in Fig. 2. They constitute the axes along which the various electric-field vectors are resolved.

C. Field Equations

For this particular four-beam case, the fundamental relations (2.1) written in the component form yield the following set of eight homogeneous equations:

$$\begin{aligned}
&x_OE_O{}^\sigma+\phi_HE_H{}^\sigma(\boldsymbol{\sigma}_O\cdot\boldsymbol{\sigma}_H)+\phi_HE_H{}^\pi(\boldsymbol{\sigma}_O\cdot\boldsymbol{\pi}_H)+\phi_QE_Q{}^\sigma(\boldsymbol{\sigma}_O\cdot\boldsymbol{\sigma}_Q)+\phi_QE_Q{}^\pi(\boldsymbol{\sigma}_O\cdot\boldsymbol{\pi}_Q)\\
&\qquad+\phi_PE_P{}^\sigma(\boldsymbol{\sigma}_O\cdot\boldsymbol{\sigma}_P)+\phi_PE_P{}^\pi(\boldsymbol{\sigma}_O\cdot\boldsymbol{\pi}_P)=0,\\
&x_OE_O{}^\pi+\phi_HE_H{}^\sigma(\boldsymbol{\pi}_O\cdot\boldsymbol{\sigma}_H)+\phi_HE_H{}^\pi(\boldsymbol{\pi}_O\cdot\boldsymbol{\pi}_H)+\phi_QE_Q{}^\sigma(\boldsymbol{\pi}_O\cdot\boldsymbol{\sigma}_Q)+\phi_QE_Q{}^\pi(\boldsymbol{\pi}_O\cdot\boldsymbol{\pi}_Q)\\
&\qquad+\phi_PE_P{}^\sigma(\boldsymbol{\pi}_O\cdot\boldsymbol{\sigma}_P)+\phi_PE_P{}^\pi(\boldsymbol{\pi}_O\cdot\boldsymbol{\pi}_P)=0,\\
&\phi_HE_O{}^\sigma(\boldsymbol{\sigma}_H\cdot\boldsymbol{\sigma}_O)+\phi_HE_O{}^\pi(\boldsymbol{\sigma}_H\cdot\boldsymbol{\pi}_O)+x_HE_H{}^\sigma+\phi_{H-Q}E_Q{}^\sigma(\boldsymbol{\sigma}_H\cdot\boldsymbol{\sigma}_Q)\\
&\qquad+\phi_{H-Q}E_Q{}^\pi(\boldsymbol{\sigma}_H\cdot\boldsymbol{\pi}_Q)+\phi_{H-P}E_P{}^\sigma(\boldsymbol{\sigma}_H\cdot\boldsymbol{\sigma}_P)+\phi_{H-P}E_P{}^\pi(\boldsymbol{\sigma}_H\cdot\boldsymbol{\pi}_P)=0,\\
&\phi_HE_O{}^\sigma(\boldsymbol{\pi}_H\cdot\boldsymbol{\sigma}_O)+\phi_HE_O{}^\pi(\boldsymbol{\pi}_H\cdot\boldsymbol{\pi}_O)+x_HE_H{}^\pi+\phi_{H-Q}E_Q{}^\sigma(\boldsymbol{\pi}_H\cdot\boldsymbol{\sigma}_Q)\\
&\qquad+\phi_{H-Q}E_Q{}^\pi(\boldsymbol{\pi}_H\cdot\boldsymbol{\pi}_Q)+\phi_{H-P}E_P{}^\sigma(\boldsymbol{\pi}_H\cdot\boldsymbol{\sigma}_P)+\phi_{H-P}E_P{}^\pi(\boldsymbol{\pi}_H\cdot\boldsymbol{\pi}_P)=0,\\
&\phi_QE_O{}^\sigma(\boldsymbol{\sigma}_Q\cdot\boldsymbol{\sigma}_O)+\phi_QE_O{}^\pi(\boldsymbol{\sigma}_Q\cdot\boldsymbol{\pi}_O)+\phi_{Q-H}E_H{}^\sigma(\boldsymbol{\sigma}_Q\cdot\boldsymbol{\sigma}_H)+\phi_{Q-H}E_H{}^\pi(\boldsymbol{\sigma}_Q\cdot\boldsymbol{\pi}_H)\\
&\qquad+x_QE_Q{}^\sigma+\phi_{Q-P}E_P{}^\sigma(\boldsymbol{\sigma}_Q\cdot\boldsymbol{\sigma}_P)+\phi_{Q-P}E_P{}^\pi(\boldsymbol{\sigma}_Q\cdot\boldsymbol{\pi}_P)=0,\\
&\phi_QE_O{}^\sigma(\boldsymbol{\pi}_Q\cdot\boldsymbol{\sigma}_O)+\phi_QE_O{}^\pi(\boldsymbol{\pi}_Q\cdot\boldsymbol{\pi}_O)+\phi_{Q-H}E_H{}^\sigma(\boldsymbol{\pi}_Q\cdot\boldsymbol{\sigma}_H)+\phi_{Q-H}E_H{}^\pi(\boldsymbol{\pi}_Q\cdot\boldsymbol{\pi}_H)\\
&\qquad+x_QE_Q{}^\pi+\phi_{Q-P}E_P{}^\sigma(\boldsymbol{\pi}_Q\cdot\boldsymbol{\sigma}_P)+\phi_{Q-P}E_P{}^\pi(\boldsymbol{\pi}_Q\cdot\boldsymbol{\pi}_P)=0,\\
&\phi_PE_O{}^\sigma(\boldsymbol{\sigma}_P\cdot\boldsymbol{\sigma}_O)+\phi_PE_O{}^\pi(\boldsymbol{\sigma}_P\cdot\boldsymbol{\pi}_O)+\phi_{P-H}E_H{}^\sigma(\boldsymbol{\sigma}_P\cdot\boldsymbol{\sigma}_H)+\phi_{P-H}E_H{}^\pi(\boldsymbol{\sigma}_P\cdot\boldsymbol{\pi}_H)\\
&\qquad+\phi_{P-H}E_H{}^\sigma(\boldsymbol{\sigma}_P\cdot\boldsymbol{\sigma}_H)+\phi_{P-H}E_H{}^\pi(\boldsymbol{\sigma}_P\cdot\boldsymbol{\pi}_H)=0,\\
&\phi_PE_O{}^\sigma(\boldsymbol{\pi}_P\cdot\boldsymbol{\sigma}_O)+\phi_PE_O{}^\pi(\boldsymbol{\pi}_P\cdot\boldsymbol{\pi}_O)+\phi_{P-H}E_H{}^\sigma(\boldsymbol{\pi}_P\cdot\boldsymbol{\sigma}_H)+\phi_{P-H}E_H{}^\pi(\boldsymbol{\pi}_P\cdot\boldsymbol{\pi}_H)\\
&\qquad+\phi_{P-Q}E_Q{}^\sigma(\boldsymbol{\pi}_P\cdot\boldsymbol{\sigma}_Q)+\phi_{P-Q}E_Q{}^\pi(\boldsymbol{\pi}_P\cdot\boldsymbol{\pi}_Q)+x_PE_P{}^\pi=0.
\end{aligned} \tag{2.4}$$

[8] Our evaluations concern the case when the incident x-ray beam is monochromatic and nondivergent.
[9] For a brief summary of the methods used, see Ref. 2, and for a detailed exposition see Ref. 10.
[10] B. Batterman and H. Cole, Rev. Mod. Phys. 36, 681 (1964).

The various scalar products of the unit vectors are given by

$$\begin{aligned}
&\boldsymbol{\sigma}_O\cdot\boldsymbol{\pi}_O=\boldsymbol{\sigma}_H\cdot\boldsymbol{\pi}_H=\boldsymbol{\sigma}_Q\cdot\boldsymbol{\pi}_Q=\boldsymbol{\sigma}_P\cdot\boldsymbol{\pi}_P=0, && \boldsymbol{\pi}_O\cdot\boldsymbol{\pi}_Q=\boldsymbol{\pi}_P\cdot\boldsymbol{\pi}_H=-\sin^2\theta=-\gamma_2,\\
&\boldsymbol{\sigma}_O\cdot\boldsymbol{\sigma}_Q=\boldsymbol{\sigma}_P\cdot\boldsymbol{\sigma}_H=1, && \boldsymbol{\pi}_O\cdot\boldsymbol{\pi}_H=\boldsymbol{\pi}_Q\cdot\boldsymbol{\pi}_P=\sin^2\theta=\gamma_2,\\
&\boldsymbol{\sigma}_O\cdot\boldsymbol{\sigma}_P=\boldsymbol{\sigma}_O\cdot\boldsymbol{\sigma}_H=\boldsymbol{\sigma}_Q\cdot\boldsymbol{\sigma}_P=\boldsymbol{\sigma}_Q\cdot\boldsymbol{\sigma}_H=0, && \boldsymbol{\pi}_O\cdot\boldsymbol{\pi}_Q=\boldsymbol{\pi}_P\cdot\boldsymbol{\pi}_H=\cos2\theta=\gamma, \qquad (2.5)\\
&\boldsymbol{\sigma}_O\cdot\boldsymbol{\pi}_Q=\boldsymbol{\sigma}_Q\cdot\boldsymbol{\pi}_O=\boldsymbol{\sigma}_P\cdot\boldsymbol{\pi}_H=\boldsymbol{\sigma}_H\cdot\boldsymbol{\pi}_P=0, && \boldsymbol{\pi}_O\cdot\boldsymbol{\sigma}_P=\boldsymbol{\pi}_O\cdot\boldsymbol{\sigma}_H=\boldsymbol{\pi}_Q\cdot\boldsymbol{\sigma}_P=\boldsymbol{\pi}_Q\cdot\boldsymbol{\sigma}_H=\cos\theta=\gamma_1,\\
& && \boldsymbol{\pi}_P\cdot\boldsymbol{\sigma}_O=\boldsymbol{\pi}_P\cdot\boldsymbol{\sigma}_Q=\boldsymbol{\pi}_H\cdot\boldsymbol{\sigma}_Q=\boldsymbol{\pi}_H\cdot\boldsymbol{\sigma}_Q=\cos\theta=\gamma_1.
\end{aligned}$$

The geometrical structure factors entering into the polarizabilities ϕ are given by the following expressions:

$$\begin{aligned}
&F_{-H}=-8f(\theta_1), && F_Q=-8f(\theta_2),\\
&F_{-Q}=-8f(\theta_2), && F_{Q-H}=+8f(\theta_1),\\
&F_{-P}=+8f(\theta_1), && F_{Q-P}=-8f(\theta_1),\\
&F_H=-8f(\theta_1), && F_P=+8f(\theta_1),\\
&F_{H-Q}=+8f(\theta_1), && F_{P-H}=-8f(\theta_2),\\
&F_{H-P}=-8f(\theta_2), && F_{P-Q}=-8f(\theta_1).
\end{aligned} \qquad (2.6)$$

By writing the parameter x in units of $|\phi_H|$, this latter value may be factored out of the homogeneous equations, and the secular equation for the four-field case under consideration takes the form

$$\begin{vmatrix}
-x_O & 0 & 0 & \gamma_1 & -1 & 0 & 0 & \gamma_1\\
0 & -x_O & \gamma_1 & \gamma_2 & 0 & -\gamma & \gamma_1 & \gamma_2\\
0 & \gamma_1 & -x_H & 0 & 0 & -\gamma_1 & -1 & 0\\
\gamma_1 & \gamma_2 & 0 & -x_H & -\gamma_1 & \gamma_2 & 0 & -\gamma\\
-1 & 0 & 0 & -\gamma_1 & -x_Q & 0 & 0 & \gamma_1\\
0 & -\gamma & -\gamma_1 & \gamma_2 & 0 & -x_Q & \gamma_1 & \gamma_2\\
0 & -\gamma_1 & -1 & 0 & 0 & \gamma_1 & -x_P & 0\\
-\gamma_1 & \gamma_2 & 0 & -\gamma & \gamma_1 & \gamma_2 & 0 & -x_P
\end{vmatrix}=0. \qquad (2.7)$$

This secular equation can now be solved for a particular set of wave points. For $x_O=x_H=x_P=x_Q=x$, we would obtain the values of x corresponding to the symmetry points of the dispersion surfaces.[11]

When the crystal is cut so that its surface is parallel to the plane of O, H, and Q, a unidirectional incident beam will excite simultaneously the symmetry points on all the dispersion surfaces. The eight roots of the secular Eq. (2.7) are

$$\begin{aligned}
x_1&=-\gamma\phi_2-2\gamma_2\phi_1,\\
x_2&=-\gamma\phi_2+2\gamma_2\phi_1,\\
x_{3,4}&=-\phi_2, \qquad (2.8)\\
x_{5,6}&=\tfrac{1}{2}[(1+\gamma)\phi_2+(\phi_2^2(1-\gamma)^2+16\phi_1^2\gamma_1^2)^{1/2}],\\
x_{7,8}&=\tfrac{1}{2}[(1+\gamma)\phi_2-(\phi_2^2(1-\gamma)^2+16\phi_1^2\gamma_1^2)^{1/2}].
\end{aligned}$$

D. Modes of Propagation

The modes of propagation for the unique roots of the secular equation are determined by substitution of the respective root into the set of homogeneous equations (2.4), and solving for the ratios of the various field components. For the degenerate roots, a perturbation technique must be employed because the multiplicity of the roots indicates that there are only six independent equations.

One of the ways in which the perturbation can be achieved is to rotate the crystal about the reciprocal-lattice vector Q; in this case the points H and P will leave the Ewald sphere, one in the outward direction and the other in the inward direction, by an amount which depends on the angle of rotation. From this rotation a small change in the magnitudes and directions of the wave vectors $\mathbf{k}_H$ and $\mathbf{k}_P$ will result; thus x_H and x_P will change slightly while x_O and x_Q will

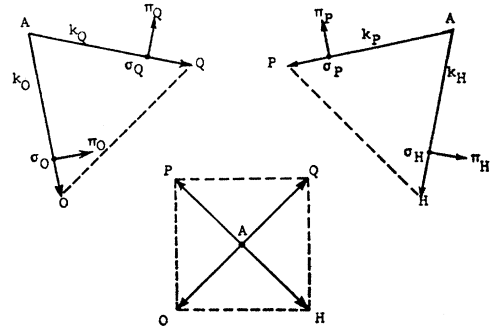

FIG. 2. Geometry of the four-beam case. Point A is the symmetry point, and O, H, P and Q are the reciprocal-lattice points. The two upper views are sections of the square pyramid normal to its base.

[11] In Sec. IV we justify this procedure.

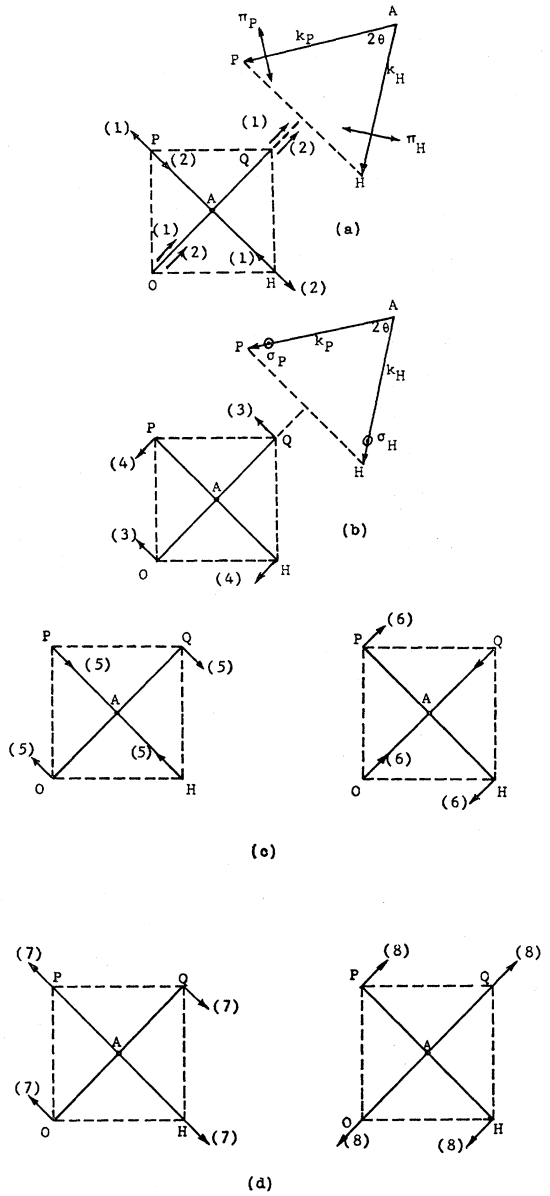

FIG. 3. The modes of propagation. (a) The arrows (1) and (2) represent the amplitude vectors associated with the eigenvalues $x=2\gamma_2\phi_1-\gamma\phi_2$ and $x=-2\gamma_2\phi_1-\gamma\phi_2$, respectively. From point A, the symmetry point, wave vectors are drawn to the reciprocal lattice points, forming a pyramid with a square base. The field vectors are shown in projection. The figure to the upper right is a section of the pyramid cut normal to the base. (b) The degenerate modes (3) and (4) associated with the eigenvalue $x=-\phi_2$. (c) The degenerate modes (5) and (6) associated with the eigenvalue $x_{5,6}$. (d) The degenerate modes (7) and (8) associated with the eigenvalue $x_{7,8}$.

remain unchanged, i.e., we can write

$$x=x_O=x_Q, \quad x_H=x+\delta, \quad x_P=x-\delta.$$

These values are substituted into the homogeneous equations which are then solved for the various field ratios, using a first-order approximation (i.e., terms δ^2 and higher are neglected). The resulting modes of propagation are shown in Fig. 3. The field components in the various modes are given by the following relations:

Mode No. 1: $E_{O1}{}^{\sigma}=E_{H1}{}^{\sigma}=E_{Q1}{}^{\sigma}=E_{P1}{}^{\sigma}=0$,
$E_{O1}{}^{\pi}=E_{H1}{}^{\pi}=E_{Q1}{}^{\pi}=E_{P1}{}^{\pi}$;

Mode No. 2: $E_{O2}{}^{\sigma}=E_{H2}{}^{\sigma}=E_{Q2}{}^{\sigma}=E_{P2}{}^{\sigma}=0$,
$E_{O2}{}^{\pi}=E_{H2}{}^{\pi}=E_{Q2}{}^{\pi}=E_{P2}{}^{\pi}$;

Mode No. 3: $E_{O3}{}^{\pi}=E_{H3}{}^{\sigma}=E_{H3}{}^{\pi}=E_{P3}{}^{\sigma}=E_{P3}{}^{\pi}=E_{Q3}{}^{\pi}=0$,
$E_{O3}{}^{\sigma}=E_{Q3}{}^{\sigma}$;

Mode No. 4: $E_{O4}{}^{\sigma}=E_{O4}{}^{\pi}=E_{H4}{}^{\pi}=E_{Q4}{}^{\sigma}=E_{Q4}{}^{\pi}=E_{P4}{}^{\pi}=0$,
$E_{P4}{}^{\sigma}=E_{H4}{}^{\sigma}$;

Mode No. 5: $E_{O5}{}^{\pi}=E_{H5}{}^{\sigma}=E_{Q5}{}^{\pi}=E_{P5}{}^{\sigma}=0$,
$E_{O5}{}^{\sigma}=-E_{Q5}{}^{\sigma}$,
$E_{H5}{}^{\pi}=-E_{P5}{}^{\pi}=-(4\gamma_1\phi_1)^{-1}[(\gamma-1)\phi_2+((\gamma-1)^2\phi_2{}^2+16\gamma_1{}^2\phi_1{}^2)^{1/2}]E_{O5}{}^{\sigma}$;

Mode No. 6: $E_{O6}{}^{\sigma}=E_{Q6}{}^{\sigma}=E_{H6}{}^{\pi}=E_{P6}{}^{\pi}=0$,
$E_{H6}{}^{\sigma}=-E_{P6}{}^{\sigma}$,
$E_{O6}{}^{\pi}=-E_{Q6}{}^{\pi}=-(4\gamma_1\phi_1)^{-1}[(\gamma-1)\phi_2+((\gamma-1)^2\phi_2{}^2+16\gamma_1{}^2\phi_1{}^2)^{1/2}]E_{H6}{}^{\sigma}$;

Mode No. 7: $E_{O7}{}^{\pi}=E_{Q7}{}^{\pi}=E_{H7}{}^{\sigma}=E_{P7}{}^{\sigma}=0$,
$E_{O7}{}^{\sigma}=-E_{Q7}{}^{\sigma}$,
$E_{H7}{}^{\pi}=-E_{P7}{}^{\pi}=-(4\gamma_1\phi_1)^{-1}[(\gamma-1)\phi_2-((\gamma-1)^2\phi^2{}_2+16\gamma_1{}^2\phi_1{}^2)^{1/2}]E_{O7}{}^{\sigma}$;

Mode No. 8: $E_{O8}{}^{\sigma}=E_{Q8}{}^{\sigma}=E_{H8}{}^{\pi}=E_{P8}{}^{\pi}=0$,
$E_{H8}{}^{\sigma}=-E_{P8}{}^{\sigma}$,
$E_{O8}{}^{\pi}=-E_{Q8}{}^{\pi}=-(4\gamma_1\phi_1)^{-1}[(\gamma-1)\phi_2-((\gamma-1)^2\phi_2{}^2+16\gamma_1{}^2\phi_1{}^2)^{1/2}]E_{H8}{}^{\sigma}$.

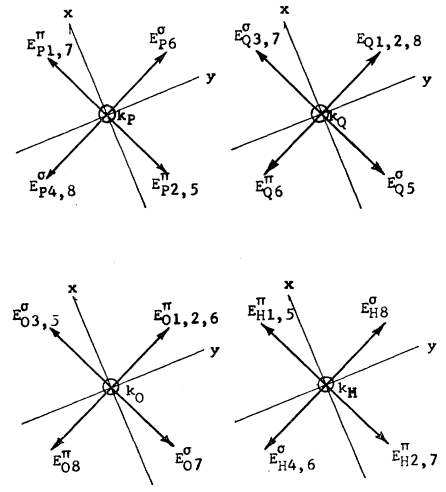

FIG. 4. Intermediate orientation of input polarization.

TABLE I. Distribution of x-ray intensity. Incident beam polarized along σ_0. Unity input $E_{Ox}^{(i)}=1$.

Mode	E_O	E_O^2	E_H	E_H^2	E_Q	E_Q^2	E_P	E_P^2	E_I^2
1	0	0	0	0	0	0	0	0	0
2	0	0	0	0	0	0	0	0	0
3	0.500	0.250	0	0	0.500	0.250	0	0	0.500
4	0	0	0	0	0	0	0	0	0
5	0.213	0.045	0.248	0.062	−0.213	0.045	−0.248	0.062	0.213
6	0	0	0	0	0	0	0	0	0
7	0.287	0.082	−0.248	0.062	−0.287	0.082	0.248	0.062	0.287
8	0	0	0	0	0	0	0	0	0

TABLE II. Distribution of x-ray intensity. Incident beam polarized along π_O. Unity input $E_{Oy}^{(i)}=1$.

Mode	E_O	E_O^2	E_H	E_H^2	E_Q	E_Q^2	E_P	E_P^2	E_I^2
1	0.250	0.062	0.250	0.062	0.250	0.062	0.250	0.062	0.250
2	0.250	0.062	−0.250	0.062	0.250	0.062	−0.250	0.062	0.250
3	0	0	0	0	0	0	0	0	0
4	0	0	0	0	0	0	0	0	0
5	0	0	0	0	0	0	0	0	0
6	0.286	0.082	−0.248	0.062	−0.287	0.082	0.248	0.062	0.287
7	0	0	0	0	0	0	0	0	0
8	0.213	0.045	0.248	0.062	−0.213	0.045	−0.248	0.062	0.213

E. Boundary Conditions

It is now necessary to evaluate the distribution of the incident intensity among the eight modes of propagation. We note that each of the four appreciable beams in the crystal is composed of eight waves originating from the eight active wave points on the surfaces of dispersion. In applying the boundary conditions, the small differences in the directions and the magnitudes of these constituent wave vectors are neglected. The electric-field amplitudes from each mode, belonging to the same beam, are superimposed. In Fig. 4 each beam ($\mathbf{k}_O$, $\mathbf{k}_H$, etc.) is perpendicular to the plane of the paper, and the field vectors comprising each beam are shown with their true relative orientation.

Unpolarized incident radiation can be considered to consist of two components linearly polarized at right angles to each other and unrelated in phase. These two polarization directions are shown as x and y in Fig. 4.

If we assume that the incident x-ray beam is linearly polarized along x, then the boundary conditions take the form

$$\sum_{\alpha=1}^{8} E_{Ox}^{(\alpha)}=E_{Ox}^{(i)},\quad \sum_{\alpha=1}^{8} E_{Oy}^{(\alpha)}=0.$$

For the diffracted beam they take the form

$$\sum_{\alpha=1}^{8} E_{nx}^{(\alpha)}=0,\quad \sum_{\alpha=1}^{8} E_{ny}^{(\alpha)}=0,$$

where $n=H$, P, and Q. The application of these conditions yields the following set of equations:

$\mathbf{k}_O$: x component: $1=E_{O3}^{\sigma}+E_{O5}^{\sigma}+E_{O7}^{\sigma}$,
y component: $0=E_{O1}^{\pi}+E_{O2}^{\pi}+E_{O6}^{\pi}+E_{O8}^{\pi}$;

$\mathbf{k}_H$: x component: $0=E_{H1}^{\pi}+E_{H2}^{\pi}+E_{H5}^{\pi}+E_{H7}^{\pi}$,
y component: $0=E_{H4}^{\sigma}+E_{H6}^{\sigma}+E_{H8}^{\sigma}$;

$\mathbf{k}_P$: x component: $0=E_{P1}^{\pi}+E_{P2}^{\pi}+E_{P5}^{\pi}+E_{P7}^{\pi}$,
y component: $0=E_{P4}^{\sigma}+E_{P6}^{\sigma}+E_{P8}^{\sigma}$;

$\mathbf{k}_Q$: x component: $0=E_{Q3}^{\sigma}+E_{Q5}^{\sigma}+E_{Q7}^{\sigma}$,
y component: $0=E_{Q1}^{\pi}+E_{Q2}^{\pi}+E_{Q6}^{\pi}+E_{Q8}^{\pi}$.

Using the relations among the field components within each mode of propagation, it is then possible to obtain the desired distribution of the incident intensity. This procedure is repeated for the incident beam polarized along the y direction. The results for each case are shown in Tables I and II, where the inputs $E_{Ox}^{(i)}$ and $E_{Oy}^{(i)}$ have been taken as unity.

F. Standing-Wave Modes and the Exit Intensities

The only modes of propagation that can contribute to the anomalous transmission of x rays are those that can form a standing-wave field in the crystal. A four-field case would seem to indicate that only modes 3 and 4 can satisfy the standing-wave criteria. Tables I and II show that mode 4 receives no energy from the

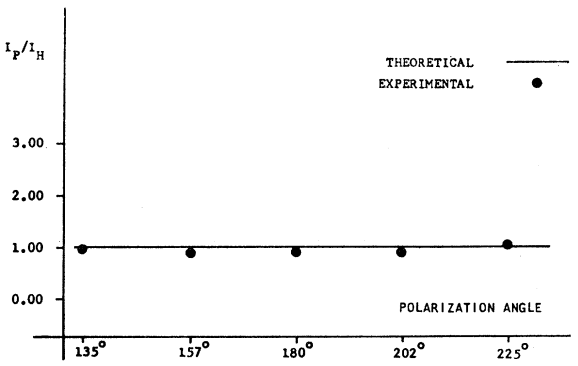

FIG. 5. Variation of the ratio I_P/I_H with polarization angle.

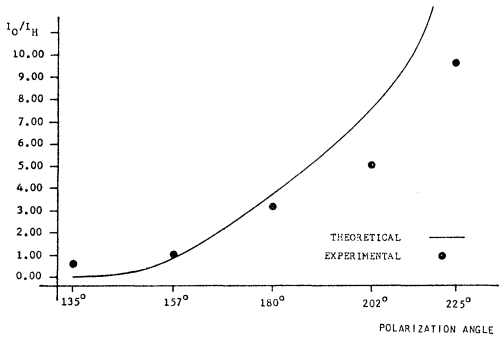

FIG. 6. Variation of the ratio I_O/I_H with polarization angle.

incident beam and therefore only mode 3 would seem to produce the anomalous transmission. Since mode 3 consists of an E_O and an E_Q field, we might be inclined to predict that (for an incident monochromatic and nondivergent x-ray beam) only two beams would leave the crystal. A series of experiments which we have performed convinced us that this prediction is not correct.

We have reexamined the modes of propagation under the assumption that the coupling among the various beams within a mode is not strong enough to prevent a pair of the consituent beams from producing the necessary standing-wave field while the remaining beams would be absorbed.[12] This coupled-pair concept treats the phenomenon of simultaneous anomalous transmission as a kind of superposition of two-field events. The application of this concept to our four-field case yields four additional standing waves. In mode 5 (Fig. 3), the two fields E_{O5} and E_{Q5} are collinear and equal in magnitude, and will therefore form a standing wave; similarly, the following pairs will form standing waves: E_{H6} and E_{P6} in mode 6, E_{O7} and E_{Q7} in mode 7, and E_{H8} and E_{P8} in mode 8. Of these, the standing waves from modes 7 and 8 have the antinodal planes coincident with the atomic planes in the crystal, and therefore they will be absorbed anomalously.

The coupled-beam concept predicts that there are four beams leaving the crystal and that each beam is polarized. The intensities for an unpolarized incident beam, as well as for an incident beam selectively polarized along five different directions, are summarized in Table III.[7]

G. Experiments

A series of experiments was carried out to examine the behavior of the intensities. The germanium crystals were in the form of circular plates 2 cm in diam and 0.5 mm thick. The incident radiation was a monochromatic x-ray beam from a copper target ($\lambda = 1.54$ Å). In order

[12] We have also investigated the possibility of obtaining standing waves formed by superposition of three or more beams. The results of our analysis were that, at least in the case under consideration, no standing waves resulting from the superposition of more than two fields can be produced.

TABLE III. Relative beam intensities.

Polarization angle	I_O	I_H	I_P	I_Q
135°	0	6.2	6.2	0
157°	4.2	5.3	5.3	4.2
180°	13.9	3.75	3.75	13.9
202°	22.5	2.95	2.95	22.5
225°	29.5	0	0	29.5
Unpolarized beam	14.8	3.1	3.1	14.8

to obtain the precise four-beam simultaneous diffraction, it is necessary first to obtain one of the diffractions, and then rotate the crystal about an axis perpendicular to the primary diffracting planes. As the crystal is rotated, the primary diffraction will be maintained and other reciprocal lattice points will be brought onto the Ewald sphere. The simultaneous event will be signaled by a sharp increase of the beam diffracted in the forward direction.[13]

The intensities of each beam were measured by a scintillation counter. The divergence of the incident beam was approximately 0.8 min of arc. The incident beam was polarized by using the anomalously transmitted beam from another perfect germanium crystal.[14] The measurements were made for each of the five polarizations listed in Table III. The results of this series of extensive experiments are shown in Figs. 5–7. In these figures we have plotted the ratios of the various beam intensities versus the polarization angles. Since we did not include absorption, we cannot expect complete agreement. We may conclude, however, that the behavior of these ratios follows the trend of our theoretical predictions.

III. SURFACE OF DISPERSION

The surfaces of dispersion are of central importance in the dynamical theory of x-ray diffraction. Up to now, with very few exceptions, such surfaces have been obtained for the case of single diffraction only. We have undertaken the determination of the dispersion surfaces

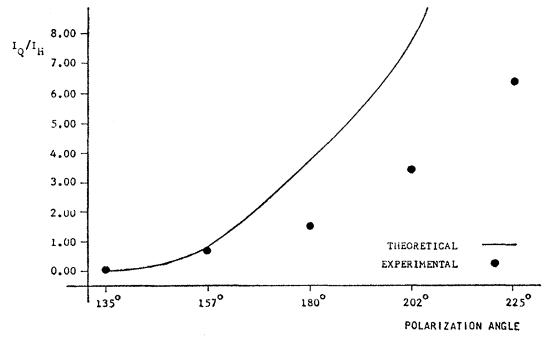

FIG. 7. Variation of the ratio I_Q/I_H with polarization angle.

[13] The procedure to be employed in this case, in particular the amount of crystal rotation, can be evaluated from the expressions developed by Cole *et al.*, Acta Cryst. 15, 138 (1962).

[14] H. Cole, J. Appl. Phys. 32, 1942 (1961).

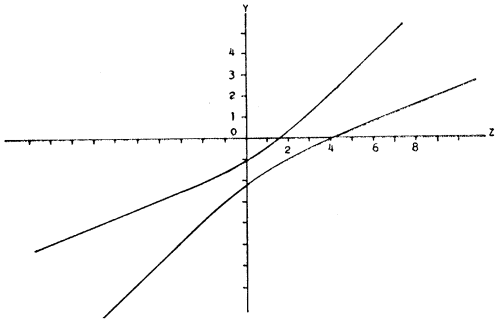

FIG. 8. Intersection of the dispersion surface and zy plane.

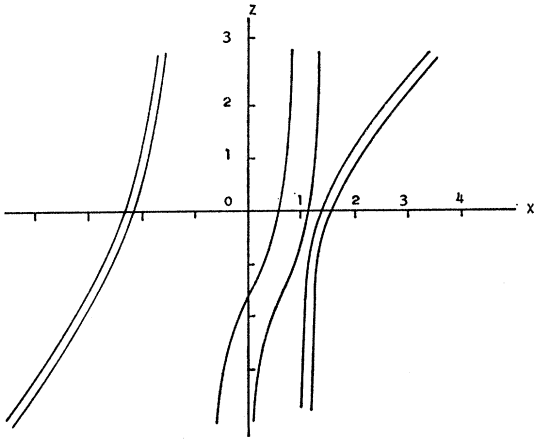

FIG. 9. Intersection of the dispersion surface and the xz plane.

for a case of the simultaneous diffraction of x rays. The case which we considered was the symmetrical three-beam case $O(000)$, $H(220)$, and $P(202)$ in germanium. The dispersion equation for this case is given by

$$\begin{vmatrix} -x_O & 0 & 1 & 0 & \gamma_3 & 0 \\ 0 & -x_O & 0 & \gamma & \gamma_4 & \gamma_2 \\ 1 & 0 & -x_H & 0 & -\gamma_3 & 0 \\ 0 & \gamma & 0 & -x_H & \gamma_4 & -\gamma_2 \\ \gamma_3 & \gamma_4 & -\gamma_3 & \gamma_4 & -x_P & 0 \\ 0 & \gamma_2 & 0 & -\gamma_2 & 0 & -x_P \end{vmatrix} = 0,$$

where the symbols have the same meaning as the corresponding symbols in Sec. II.

Since the three quantities x_O, x_H, and x_P are measured along the vectors $\mathbf{k}_O$, $\mathbf{k}_H$, and $\mathbf{k}_P$ emanating from an active wave point on the surface of dispersion, they can be considered as segments lying along the axes of an oblique coordinate system. As the position of the active wave point varies over the dispersion surface, the relative orientation of these three reference axes will vary also. However, considering the scale employed and realizing that the dispersion surfaces are effectively at a very great distance from the reciprocal-lattice points, the orientation of the axes can be considered as constant.

If the determinant of the last equation is evaluated and the resulting equation transformed to the Cartesian form, the following dispersion equation is obtained:

$$\begin{aligned}&(x^4\gamma^2+2\gamma\delta_1x^3y+\delta_1^2x^2y^2)(x^2\delta_2^2+y^2\delta_3^2+z^2\delta_4^2+2\delta_2\delta_3xy+2\delta_2\delta_4xz+2\delta_3\delta_4yz)-x^2(x\gamma+\delta_1y)(x\delta_2+y\delta_3\\&+z\delta_4)(\gamma_2^2+\gamma_3^2+\gamma_4^2)-x(x^2\gamma^2+2\gamma\delta_1xy+\delta_1^2y^2)(x\delta_2+y\delta_3+z\delta_4)(\gamma_2^2+\gamma_3^2+\gamma_4^2)-x(x\gamma+\delta_1y)(x^2\delta_2^2\\&+y^2\delta_3^2+z^2\delta_4^2+2\delta_2\delta_3xy+2\delta_2\delta_4xz+2\delta_3\delta_4yz)(1+\gamma^2)+2x(x\gamma+\delta_1y)(x\delta_2+y\delta_3+z\delta_4)(\gamma\gamma_2^2+\gamma_3^2-\gamma\gamma_4^2)\\&+x^2\gamma^2+(x^2\gamma^2+2\gamma\delta_1xy+\delta_1^2y^2)\gamma^2+(x^2\delta_2^2+y^2\delta_3^2+z^2\delta_4^2+2\delta_2\delta_3xy+2\delta_2\delta_4xz+2\delta_3\delta_4yz)\gamma^2\\&+2x(x\gamma+\delta_1y)(2\gamma_4^2\gamma_2^2+\gamma^2)+x(x\delta_2+y\delta_3+z\delta_4)(\gamma^2\gamma_3^2+\gamma_2^2+\gamma_4^2)+(x\gamma+\delta_1y)(x\delta_2+y\delta_3\\&+z\delta_4)(\gamma^2\gamma_3^2+\gamma_2^2+\gamma_4^2)-2x(\gamma^3+\gamma^2)-2(x\gamma+\delta_1y)(\gamma^3+\gamma^2)-2(x\delta_2+y\delta_3+z\delta_4)(\gamma\gamma_2^2+\gamma^2\gamma_3^2-\gamma\gamma_4^2)+4(\gamma^3-\gamma_2^2\gamma_4^2)=0.\end{aligned}$$

This is the equation of the dispersion sheets for the case under consideration.

To obtain some idea of the actual form of the dispersion surface, we considered the intersections of the surface with the three coordinate planes[15,16]

The plots of the equations which represent these intersections are shown in Figs. 8–10. From these three curves it is possible to construct the general shape and the configuration of the surfaces of dispersion for the case under consideration. Figure 11 is a simplified representation of these surfaces. It can be seen that the surfaces of dispersion for this case of simultaneous diffraction are somewhat similar in shape to the surfaces for the case of the single diffraction in that in both cases there are pairs of closely spaced sheets, each with a general hyperboloidal curvature.[17]

IV. DOMINANT WAVE POINTS ON THE SURFACE OF DISPERSION

The modes of propagation of the electromagnetic waves which have been discussed here in Sec. II[18] have been determined for a restricted set of wave points only, viz., for the symmetry points of the dispersion surface. We will now give an argument which indicates

[15] A computer was used to evaluate the coefficients of the necessary equations; for details see Ref. 16.

[16] Andrew Dalisa, Ph.D. thesis, Adelphi University, 1967 (unpublished).

[17] The separability of the dispersion equation into a product of lower-order determinants is a problem of considerable interest. We have investigated this problem to some extent, and found that any coplanar case of simultaneous anomalous transmission will possess a factorable dispersion equation. However, we are convinced that the noncoplanar cases, such as $O(000)$, $H(220)$, $P(202)$, are indications that the dispersion equation cannot be factored. (See A. Dalisa, Ref. 16.)

[18] See also Ref. 3.

that these symmetry points actually play a dominant role in the anomalous transmission. The discussion of this problem that is presented below concerns one of the three-field cases.

The three fundamental equations for the three-field case $O(000)$, $H(220)$, and $P(202)$ are

$$-x_O\mathbf{E}_O=\phi_H\mathbf{E}_H-\lambda_O(\lambda_O\cdot\mathbf{E}_H)+\phi_P\mathbf{E}_O-\lambda_O(\lambda_O\cdot\mathbf{E}_H),$$
$$-x_H\mathbf{E}_H=\phi_H\mathbf{E}_O-\lambda_H(\lambda_H\cdot\mathbf{E}_O)+\phi_{H-P}\mathbf{E}_P-\lambda_H(\lambda_H\cdot\mathbf{E}_P),$$
$$-x_P\mathbf{E}_P=\phi_P\mathbf{E}_O-\lambda_P(\lambda_P\cdot\mathbf{E}_O)+\phi_{P-H}\mathbf{E}_H-\lambda_P(\lambda_P\cdot\mathbf{E}_H).$$

Introducing three unit vectors $\mathbf{b}_O$, $\mathbf{b}_H$, and $\mathbf{b}_P$ along the field components $\mathbf{E}_O$, $\mathbf{E}_H$, and $\mathbf{E}_P$, respectively, and scalar multiplying the above three equations by the respective unit vectors, yields the following results:

$$-x_O\mathbf{E}_O=\phi_H\mathbf{E}_H\cos(\mathbf{b}_O,\mathbf{E}_H)+\phi_H\mathbf{E}_P\cos(\mathbf{b}_O,\mathbf{E}_P),$$
$$-x_H\mathbf{E}_H=\phi_H\mathbf{E}_O\cos(\mathbf{b}_H,\mathbf{E}_O)-\phi_H\mathbf{E}_P\cos(\mathbf{b}_H,\mathbf{E}_P),$$
$$-x_P\mathbf{E}_P=\phi_H\mathbf{E}_O\cos(\mathbf{b}_P,\mathbf{E}_O)-\phi_H\mathbf{E}_H\cos(\mathbf{b}_P,\mathbf{E}_H),$$

where use has been made of the following relations among the polarizabilities:

$$\phi_H=\phi_{-H},\quad \phi_P=\phi_{-P},\quad \phi_{H-P}=\phi_{P-H},$$
$$\phi_H=\phi_P,\quad \phi_H=-\phi_{H-P}.$$

The above set of equations will be solved for the case when certain of the field vectors are parallel; this is the first condition that a standing-wave field be formed.

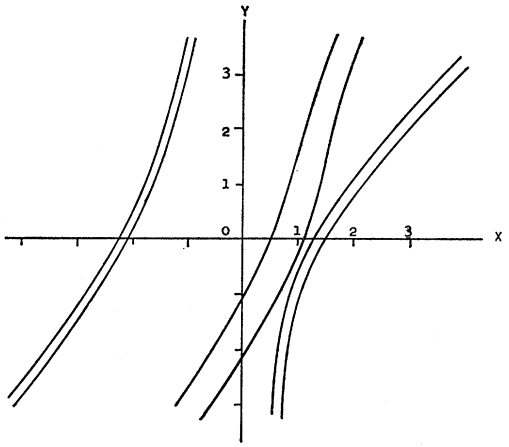

FIG. 10. Intersection of the dispersion surface and the xy plane.

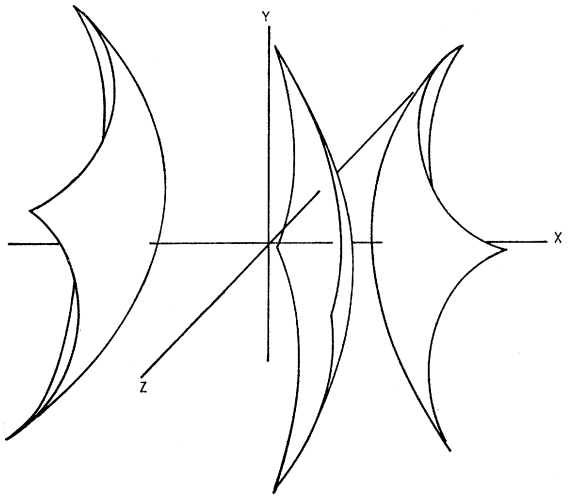

FIG. 11. Three-beam dispersion surfaces. This is a representation of the three dimensional dispersion surfaces for the three-beam case $O(000)$, $H(220)$, and $P(202)$. Each of the sheets shown above is actually accompanied by a closely spaced additional sheet.

When $\mathbf{E}_H$ is parallel to $\mathbf{E}_O$,

$$E_H/E_O=-(\phi_H+x_O)/(\phi_H+x_H);$$

when $\mathbf{E}_H$ is parallel to $\mathbf{E}_P$,

$$E_H/E_P=-(\phi_H+x_P)/(\phi_H+x_H);$$

and when $\mathbf{E}_O$ is parallel to $\mathbf{E}_P$ we obtain

$$E_O/E_P=(\phi_H+x_P)/(\phi_H+x_O).$$

In addition to the requirement that the respective field vectors be parallel in order for the anomalous transmission to occur, the above ratios have to be equal to unity. We see that this can only occur when

$$x_O=x_H=x_P.$$

This restriction is exactly the same under which the analysis of the anomalous transmission has been carried out for a three-beam case[2] and the same type of condition ($x_O=x_H=x_P=x_Q$) was used in the analysis of the four-field case in Sec. II above.

ACKNOWLEDGMENT

Certain parts of this work have been discussed with E. J. Saccocio, and the authors thank him for his contributions.